Downloaded from orbit.dtu.dk on: May 13, 2025

DTU Library

Selective enzymatic release and gel formation by crosslinking of feruloylated glucurono-arabinoxylan from corn bran

Munk, Line; Muschiol, Jan; Li, Kai; Liu, Ming; Perzon, Alixander; Meier, Sebastian; Ulvskov, Peter; Meyer, Anne S.

Published in:
ACS Sustainable Chemistry & Engineering

Link to article, DOI:
10.1021/acssuschemeng.0c00663

Publication date:
2020

Document Version
Peer reviewed version

Link back to DTU Orbit

Citation (APA):
Munk, L., Muschiol, J., Li, K., Liu, M., Perzon, A., Meier, S., Ulvskov, P., & Meyer, A. S. (2020). Selective enzymatic release and gel formation by crosslinking of feruloylated glucurono-arabinoxylan from corn bran. *ACS Sustainable Chemistry & Engineering*, *22*(8), 8164-8174. https://doi.org/10.1021/acssuschemeng.0c00663

General rights
Copyright and moral rights for the publications made accessible in the public portal are retained by the authors and/or other copyright owners and it is a condition of accessing publications that users recognise and abide by the legal requirements associated with these rights.

- Users may download and print one copy of any publication from the public portal for the purpose of private study or research.
- You may not further distribute the material or use it for any profit-making activity or commercial gain
- You may freely distribute the URL identifying the publication in the public portal

If you believe that this document breaches copyright please contact us providing details, and we will remove access to the work immediately and investigate your claim.

ACS Sustainable Chemistry & Engineering

DTU DTU Library

Article

Selective enzymatic release and gel formation by cross-linking of feruloylated glucurono-arabinoxylan from corn bran

Line Munk, Jan Muschiol, Kai Li, Ming Liu, Alixander Perzon, Sebastian Meier, Peter Ulvskov, and Anne S Meyer

ACS Sustainable Chem. Eng., **Just Accepted Manuscript** • DOI: 10.1021/acssuschemeng.0c00663 • Publication Date (Web): 11 May 2020

Downloaded from pubs.acs.org on May 18, 2020

Just Accepted

"Just Accepted" manuscripts have been peer-reviewed and accepted for publication. They are posted online prior to technical editing, formatting for publication and author proofing. The American Chemical Society provides "Just Accepted" as a service to the research community to expedite the dissemination of scientific material as soon as possible after acceptance. "Just Accepted" manuscripts appear in full in PDF format accompanied by an HTML abstract. "Just Accepted" manuscripts have been fully peer reviewed, but should not be considered the official version of record. They are citable by the Digital Object Identifier (DOI®). "Just Accepted" is an optional service offered to authors. Therefore, the "Just Accepted" Web site may not include all articles that will be published in the journal. After a manuscript is technically edited and formatted, it will be removed from the "Just Accepted" Web site and published as an ASAP article. Note that technical editing may introduce minor changes to the manuscript text and/or graphics which could affect content, and all legal disclaimers and ethical guidelines that apply to the journal pertain. ACS cannot be held responsible for errors or consequences arising from the use of information contained in these "Just Accepted" manuscripts.

is published by the American Chemical Society. 1155 Sixteenth Street N.W., Washington, DC 20036

Published by American Chemical Society. Copyright © American Chemical Society. However, no copyright claim is made to original U.S. Government works, or works produced by employees of any Commonwealth realm Crown government in the course of their duties.

Selective enzymatic release and gel formation by cross-linking of feruloylated glucurono-arabinoxylan from corn bran

Line Munk[1,‡], Jan Muschiol[1,‡], Kai Li[1], Ming Liu[1], Alixander Perzon[2], Sebastian Meier[3], Peter Ulvskov[2], Anne S. Meyer[1,*]

[1]Protein Chemistry and Enzyme Technology, DTU Bioengineering, Department of Biotechnology and Biomedicine, Technical University of Denmark, Søltofts Plads 221, DK-2800 Kgs. Lyngby, Denmark.

[2]Department of Plant and Environmental Sciences, University of Copenhagen, Thorvaldsensvej 40, DK-1871 Frederiksberg C, Denmark.

[3]Department of Chemistry (DTU Chemistry), Technical University of Denmark, Kemitorvet 207, DK-2800 Kgs. Lyngby, Denmark.

*Corresponding author: e-mail asme@dtu.dk (Anne S. Meyer), postal address as above.

‡These authors contributed equally.

ABSTRACT

Corn bran is a major agro-industrial byproduct from corn starch processing. The bran is particularly rich in highly substituted feruloylated glucuronoarabinoxylan (FGAX). Yet, due to its recalcitrance to biocatalytic degradation, corn bran FGAX is currently not utilized in biorefinery processes. Here, we report selective enzymatic extraction of both single, and double-stranded high-molecular-weight FGAX molecules from corn bran using a bacterial, glucuronoyl-specific glycoside hydrolase family 30 endo-1,4-β-xylanase (EC 3.2.1.8) from *Dickeya chrysanthemi* (DcXyn30). The enzymatic extraction using DcXyn30 was optimized with respect to temperature, pH, and time to maximize yields of high-molecular-weight polysaccharides. Examination of the enzymatically extracted FGAX using SEC, HPAEC, LC-MS, and NMR analysis (after acid or alkaline hydrolysis) revealed that both single-stranded and double-stranded FGAX were extracted, since diferulate-linkages were present in the extracted FGAX. Furthermore, the NMR-analysis indicated presence of 1,5-linked arabinan dimers suggesting that some of the xylopyranosyl residues in the extracted FGAX contained arabinofuranosyl-arabinofuranosyl substitutions in addition to a significant amount of classical doubly-arabinose substitutions. Laccase treatment of the extracted FGAX produced strong hydrogels via oxidative, covalent feruloyl-cross-linking. At pH 6.5 the *Myceliophthora thermophila* derived laccase produced significantly faster cross-linking kinetics than the laccase from *Pleurotus ostreatus* as measured rheologically. The data reveal novel insight into corn bran FGAX chemistry and provide a new direction for enzyme-assisted upgrading of corn bran for valuable functional hydrogel applications.

KEYWORDS: glycoside hydrolase family 30 xylanase; dehydrodiferulates; laccase; hydrogel

Introduction

Corn bran is an agro-industrial residue stream resulting from corn starch processing. The corn bran consists of the hulls of the maize kernels (pericarp and seed coat), and make up approx. 5% of the total kernel weight.[1] Based on recent data on global corn production (1101.2 million metric tons in 2018/2019)[2] the annual co-processing production of corn bran amounts to approx. 55 million metric tons per year. The bran is mainly used as an animal feed supplement due to its high insoluble fiber content (up to 86% (w/w)), which mainly consists of complex hemicellulose polysaccharides, notably highly substituted xylan.[3] Detailed analyses of corn bran xylan have revealed that the xylan backbone is heavily substituted with arabinosyl residues, and both mono- and di-substituted xylosyl residues with substitutions at positions O2 and/or O3 are present.[4] In addition, presence of 4-*O*-methyl-glucuronoyl, L- galactosyl and oligomeric arabinosyl substitutions,[5–8] as well as and acetylation of the xylan backbone at O2 and O3 of the xylosyl moieties, and esterification of the arabinosyl residues with ferulic acid at O5 have been described in the literature.[9–11] Hence, corn bran xylan is referred to as feruloylated glucuronoarabinoxylan (FGAX). The reported ferulic acid content of corn bran is 33 mg/g insoluble fibre, which is almost five times higher than that of other cereal brans (for wheat and barley typical levels are ~7 mg/g insoluble fibre).[12] The feruloyl substitutions make corn bran FGAX attractive as a source of potential antioxidant and prebiotic oligomers that may be applied in foods.[13–15] Alternatively, the FGAX can be used in functional or structural material applications since the feruloylated chains can be covalently cross-linked to diferulates (dehydrodiferulates, DiFAs) via oxidative enzymatic catalysis using either laccase or peroxidase to form strong hydrocolloid gels.[16,17] Classical chemical extraction methods of xylan from corn bran usually involve use of high concentrations of HCl or NaOH and high temperatures (up to 100°C) – methods that are

now considered inexpedient and which furthermore may lead to saponification of the ester modifications of the xylan.[4] Rapid, microwave-assisted hydrothermal extraction methods lead to the formation of unwanted byproducts such as furfural.[18] More recently, the extraction of hemicellulose from wheat bran by subcritical water (pressurized hot water up to 160°C) was shown to result in high yields and to preserve the valuable feruloylations in extracted FGAX, but the methodology also led to significant co-extraction of β-glucans and starch.[19,20] Therefore, it would be highly desirable to establish mild selective enzymatic extraction methods for FGAX from corn bran at low temperatures and moderate pH values, i.e. methods not requiring use of hazardous chemicals and not producing undesirable byproducts.

The less substituted xylans from other cereal sources are easily degraded by microbial endo-xylanases categorized in glycoside hydrolase (GH) families 10 and 11, and many such endo-xylanases, including inhibitor-resistant versions, have been commercially available for a decade and are of significance in baking and biofuel processes.[21,22] In contrast, the recalcitrance of raw corn bran towards enzymatic hydrolysis has hampered industrial biorefining of corn bran glucuronoarabinoxylans for creation of products for higher value applications.[23] Hence, in the native, highly substituted corn bran arabinoxylan there are essentially no regions of unsubstituted xylosyl residues available for recognition and cleavage by the GH10 and GH11 xylanases. However, endo-xylanases belonging to subfamily 8 of GH family 30 (GH30_8) have a glucuronosyl (GlcA) or 4-*O*-methyl-GlcA residue as recognition site,[24] and have been described to be active on corn xylan.[25] The hitherto described GH30_8 xylanases will thus catalyze hydrolytic cleavage of the xylan backbone at the second glycosidic linkage next to the GlcA branching (counted from the reducing end).[26,27] Based on this rare recognition site of GH30_8 xylanases, we hypothesized that high-molecular weight FGAX could be selectively extracted from corn bran via GH30_8 xylanase catalysis, and in turn, that such extracted FGAX could be

cross-linked via oxidative enzyme catalyzed formation of DiFAs to form hydrogels for novel food or material science applications. A number of GH30 xylanases originating from bacteria and fungi have been described, several of them recently, e,g. from *Bacillus* sp. BP-7,[28] *B. substilis*,[29] *B. licheniformis*,[30] *Clostridium acetobutylicum*,[31] *C. papyrosolvens*,[32] *Streptomyces turgidiscabies*,[33] *Talaromyces cellulolyticus*,[34] *Thermothelomyces thermophila*[35] (synonym *Myceliophthora thermophila*), and *Trichoderma reesei*[36]. However, in particular the endo-xylanase, DcXyn30, from *Dickeya chrysanthemi* (previously known as *Erwinia chrysanthemi* pv. *zeae* or *Dickeya zeae*)[26,27,37–40] caught our attention, because *D. chrysanthemi* is a maize pathogen.[40–43] Although this pathogenicity has been known for almost 60 years,[44] the reactivity of DcXyn30 towards corn bran FGAX has to our knowledge not been reported. Here, we show the usefulness of DcXyn30 for controlled enzymatic extraction of soluble and high-molecular weight FGAX polysaccharides from corn bran and demonstrate the applicability of the extracted FGAX molecules to form hydrogels via laccase-catalyzed cross-linking of the feruloyl residues.

Materials and Methods

Materials. The raw corn bran was supplied by Archer Daniel Midlands Co. (Decatur, IL, USA) and destarched as previously described.[45] Subsequently, the material was ball milled (MM-200, Retsch GmbH, Haan, Germany) with a frequency of 30 s^{-1} for 3 min. The composition of the raw material was determined according to the laboratory analytical procedure from the US National Renewable Energy Laboratory.[46] All other chemicals were at least of analytical grade and were used without further treatment or purification, unless stated otherwise.

Cloning, expression and purification of the DcXyn30 enzyme. The protein sequence of DcXyn30 was retrieved from the GenBank database (accession no. ACZ76867.1). The signal

peptide was detected using the SignalP server 4.1[47] and the amino acid sequence without signal peptide was submitted to GenScript (Piscataway, NJ) for synthesis of a codon-optimized gene for expression in *Escherichia coli*. Subcloning into pPAL7 (Bio-Rad Laboratories Inc., Hercules, CA, USA) using the HindIII and XhoI restriction sites was carried out by GenScript. The resulting plasmid, pPAL7_DcXyn30, was transformed into *E. coli* DH5α for maintenance and into *E. coli* BL21 (DE3) for expression using Mix&Go competent cells (Zymo Research, Irvine, CA, USA). The gene encoding the enzyme was expressed in a simplified auto-induction medium (6 g/L Na_2HPO_4, 3 g/L KH_2PO_4, 20 g/L tryptone, 5 g/L yeast extract, 5 g/L NaCl, 0.6% (v/v) glycerol, 0.05% (w/v) glucose, 0.2% (w/v) lactose) containing 50 µg/ml ampicillin as selection marker. To this end, 5 ml of a pre-culture were inoculated into 400 mL of medium in a 2 L-Erlenmeyer flask with baffles and incubated for 2 h at 37°C and 160 rpm. Afterwards, the temperature was adjusted to 20°C and the cultivation was continued overnight. The cells were harvested by centrifugation (4500 *g*, 10 min) and either lysed by ultrasound (0.6 cycle, 100% amplitude on a UP400S, Hielscher Ultrasonics GmbH, Teltow, Germany) or by a bench-top high-pressure homogenizer using one passage at 40 mbar, followed by a passage at 1 bar ('Pressure Cell' Homogenizer, Stansted Fluid Power Ltd, Essex, UK). The cell debris was removed by centrifugation at 20,000 *g* for 20 min at 4°C. The enzyme was purified using the Profinity eXact™ Fusion-Tag System (Bio-Rad Laboratories Inc.) following the manufacturer's instructions for FPLC system assisted purification (ÄKTA purifier, GE Healthcare, Uppsala, Sweden). Re-loading of the flow-through up to five times increased the yield of enzyme. Afterwards the enzyme containing fractions were either collected and concentrated to 2.5 mL followed by desalting using the gravity protocol on PD-10 columns as indicated in the manual (GE Healthcare) or desalted directly without a prior concentration step using five HiTrap Desalting columns (each 5 ml) that were connected in series to the ÄKTA purifier following the

manufacturer's manual (GE Healthcare). Purity was checked by SDS-PAGE (Mini-PROTEAN® TGX™ Precast Gels, Bio-Rad) and the protein concentration was determined using a commercial Bradford assay kit (Roti®-Nanoquant, Carl Roth GmbH + Co. KG, Karlsruhe, Germany) with bovine serum albumin as calibration standard.

Optimization of the FGAX extraction process. A 3-level full factorial design was carried out to establish optimal conditions in terms of pH and temperature for the activity of DcXyn30 on the destarched corn bran at 10% dry matter (DM) concentration. Based on preliminary experiments the enzyme dose was set to 0.010 mg/ml. Each variable (pH and temperature) was considered at three levels including a center point (in triplicates), which represented the midpoint of each factor range. Based on preliminary experiments, the levels were set to pH 4 - 7 and 25 - 65°C (pH 5.5, 45°C as center point) giving a total of 12 experiments. The release of FGAX was observed over 60 min by measuring reducing ends in the supernatant with xylose as standard. Samples taken after 60 min were also analyzed by size exclusion chromatography (SEC). The response values for the factorial design were given as the maximal release after 60 min in terms of reducing ends and area of the elution peak from 5 kDa – 110 kDa according to pullulan standards. The statistical design program JMP 14 (SAS Institute Inc., Cary, NC, USA) was used as an aid to statistically design the factorial experiments and to fit and analyze the data by multiple linear regression. Significance of the results was established at $p < 0.05$.

Extraction of soluble, high-molecular weight FGAX. FGAX polysaccharides were extracted from 10% DM destarched corn bran at pH 5.5 at 45 °C for 2 h with DcXyn30 at 0.010 mg/ml under gentle shaking. The pH in the slurry was adjusted with 0.1 M HCl. The supernatant was collected after 20 min of centrifugation at 4400 rpm. The pellet was washed in Milli-Q water and the supernatants were pooled after centrifugation. The resulting extract was left overnight to

precipitate in 90% ethanol. The precipitate was collected after centrifugation for 20 min at 4400 rpm and dried overnight at 40 °C.

Characterization of the extracted FGAX. All characterizations of the enzymatically extracted FGAX were carried out using a solution of 2% (w/v), which was prepared by dissolving the precipitated dried extract in pH-adjusted water (pH 5.5) followed by centrifugation for 5 min at 14,000 *g* to remove insoluble material. For determination of the molecular weight distribution of the FGAX extract before and after precipitation SEC was performed using an Ultimate iso-3100 SD pump with a WPS-3000 sampler (Dionex, ThermoFisher Scientific, Waltham, MA, USA) connected to an RI-101 refractive index detector (Showa Denko K.K., Tokyo, Japan). 100 µL of the sample was loaded on a Shodex SB-806 HQ GPC column (300 x 8 mm) equipped with a Shodex SB-G guard column (50 mm x 6 mm) (Showa Denko K.K.). Elution was performed with 100 mM sodium acetate at a flow rate of 0.5 mL/min at 40°C. Pullulan standards were used as reference molecular weight standards.

Monosaccharide composition was determined as previously described using 4% H_2SO_4 hydrolysis for 1 hour and analysis by high-performance anion exchange chromatography (HPAEC) with pulsed amperometric detection.[45] Ferulic acid (FA) and diferulic acids (diFAs) were identified and quantified by LC-MS on a Dionex UltiMate 3000 UHPLC system (Thermo Fischer Scientific, Sunnyvale CA, USA) connected to an ESI-iontrap (model AmaZon SL, Bruker Daltonics, Bremen, Germany). For FA and DiFA determination, the samples were saponified with 1 M NaOH overnight at 25ºC in absence of O_2. Then, pH was lowered to pH <2 and 25% (v/v) acetonitrile was added to the samples prior to LC-MS analysis. 5 µL sample were injected onto a Hypersil Gold Phenyl column (150 mm × 2.1 mm, 3 μm; Thermo Fisher Scientific). The chromatography on the Dionex UltiMate 3000 UPLC was operated at 0.4 mL/min at 40°C with a three-eluent system with elution using A: 0.1% formic acid in water;

eluent B: acetonitrile; eluent C: water as follows: 0 min, 10% A/0% B/90% C; 0 – 15 min, linear gradient to 10% A/50% B/40% C; 15 – 20 min, isocratic 10% A/50% B/40% C; 20 – 25 min, isocratic 10% A/0% B/90% C. The electrospray was operated in negative scan mode using a target mass of 400 *m/z* with a scan range from 100 to 2000 *m/z* with parameter settings as follows: capillary voltage 4.5 kV, end plate offset 0.5 kV, nebulizer pressure 3.0 bar, dry gas flow 12.0 L/min, dry gas temperature 280°C. FA was quantified by ferulic acid standard curves at 280 nm. DiFAs were identified by a combination of MS and UV spectra.[48,49] Response factors from Waldron et al.[48] were used to quantify the DiFAs.[50]

Acetate content was determined using the Acetic Acid Assay Kit (Acetate Kinase Analyser Format) from Megazyme (Bray, Ireland) according to the manufacturer's manual.

NMR spectra were recorded on lyophilized, enzymatically extracted FGAX after precipitation after re-dissolution in 0.6 ml D_2O. All spectra were acquired at 50°C using a Bruker Avance III 800 MHz spectrometer (Bruker, Fällanden, Switzerland) equipped with a TCI cryoprobe. The acquired spectra included a 1D proton spectra sampling 16384 complex data point during an acquisition time of 1.3 seconds. Homo- and heteronuclear 2D NMR spectra were additionally acquired. The 2D NMR spectra included TOCSY with a 10 kHz spin lock field that was applied for 60 ms (1024 × 256 complex data points with 213 ms and 53 ms acquisition times) and NOESY with a mixing time of 300 ms (likewise with 1024 × 256 complex data points and 213 ms and 53 ms acquisition times). The homonuclear spectra employed pre-saturation for the suppression of any residual water signal. Heteronuclear ^{1}H-^{13}C-HSQC spectra were acquired sampling 2048(^{1}H)×256(^{13}C) complex data points around a ^{13}C carrier offset of in the 75 ppm and employing a spectral width of 80 ppm in the ^{13}C dimension to sample ^{13}C signal for 16 ms and ^{1}H signal for 160 ms. ^{1}H-^{13}C-HSQC TOCSY spectra were acquired sampling 512(^{1}H)×256(^{13}C) complex data points around a ^{13}C carrier offset of in the 75 ppm and

employing a spectral width of 80 ppm in the ^{13}C dimension to sample ^{13}C signal for 16 ms and ^{1}H signal for 128 ms. In addition, ^{1}H-^{13}C-HMBC spectra were acquired sampling 2048(^{1}H)×400(^{13}C) complex data points around a ^{13}C carrier offset of in the 100 ppm and employing a spectral width of 200 ppm in the ^{13}C dimension to sample ^{13}C signal for 10 ms and ^{1}H signal for 200 ms. The sample was subsequently saponified for 3 h in 0.1 M NaOH at 45°C in the dark and the same suite of NMR spectra was acquired on the saponified sample. A 1,5-α-L-arabinan (Megazyme) was dissolved in D_2O and a high-resolution HSQC spectrum for the sample was acquired serving as a reference standard. Assignment of molecular species was aided by the acquired assignment spectra as well as by literature data[51,52] for chemical shift assignments in arabinoxylans. All spectra were processed with ample zero filling in all dimensions using Topspin 4.0.6 (Bruker, Fällanden, Switzerland). Quantitative estimates for the prevalence of different groups was likewise obtained by integration.

FGAX extract-based hydrogel formation. Hydrogel formation by laccase catalyzed cross-linking of FAs in the extracted FGAX was carried out in 2% FGAX solutions in water at pH 6.5.

The laccases were fungal laccases derived from the ascomycete *Myceliophthora thermophila* (Mt) and the basidiomycete *Pleurotus ostreatus* (Po), respectively. The Mt laccase, MtL, was donated by Novozymes A/S (Bagsværd, Denmark) and the Po laccase, PoL was purchased from Sigma-Aldrich (St. Louis, MO). Both laccases were lyophilized preparations that were kept frozen at -20°C until use. For cross-linking, the FGAX reaction mixture was in each case mixed with the laccase to give a laccase dose of 0.4 U/ml (syringaldazine units at pH 5.0), equivalent to 0.33 nkat/mg FGAX, in order to obtain gelation within a time frame of 60 min. Laccase activity was determined by monitoring the oxidation of syringaldazine (from Sigma-Aldrich (St. Louis, MO) at 530 nm ($\varepsilon = 6.5 \cdot 10^4$ M^{-1} cm^{-1}) during reaction at 25°C. The standard assay reaction mixture contained 25 μM syringaldazine, 10% (v/v) ethanol, 25 mM sodium acetate (pH 5.0) and

a suitable amount of enzyme to produce a linear absorbance increase within 5 minutes. Enzyme activity was expressed in units (U), where one l U was defined as the amount of enzyme required to catalyze conversion of 1 μmol of substrate per minute at the assay reaction conditions (1 U = 16.67 nkat). In practice, the enzyme catalyzed oxidative cross-linking (i.e. FGAX gelation) was initiated by adding laccase to the FGAX solution which was then immediately transferred to the rheometer. The rheological analyses were based on small angle measurements on 40 mm, 0.9767° cone plate with solvent trap in a Discovery HR-3 Rheometer (TA Instruments, New Castle, DE, USA). Time sweeps were recorded for 4000 s at a strain of 0.6% and a frequency of 1 Hz. Measurements were performed in triplicates within the viscoelastic region at 25ºC. The simultaneous diFA formation and FA consumption were determined by LC-MS as detailed above. Samples for LC-MS analysis were taken during the laccase reaction at set time points from 0 – 140 min, inactivated, and saponified in 1 M NaOH as described above.

Molecular substrate docking. For preparation of the substrate docked DcXyn30 the only crystal structure with a ligand bound (PDB: 2Y24)[27] was loaded into YASARA Structure (Version 19.11.2, YASARA Biosciences GmbH, Vienna, Austria).[53] One of the ligands bound in the active site (imidazole) was deleted and the second ligand bound (2^2-(4-*O*-methyl-α-D-glucuronyl)-xylotriose) was elongated with a fourth xylose residue at the reducing end using the YASARA *Build* function. The resulting complex was energy-minimized using the built-in minimization function (and the result was used to prepare Figure 4A). The acetylated ligand was created by deleting one water molecule in the tunnel close to the active site and the respective acetyl residue was built on C2 of the xylose in subsite –1 as described above. Subsequent energy minimization resulted in the complex used to prepare Figure 4B. Ray-traced screenshots for the figures were made using the in-build POV-Ray (Persistence of Vision Pty. Ltd., Williamstown, Victoria, Australia; http://www.povray.org/) function of YASARA.

Results and Discussion

Extraction of soluble FGAX. The enzymatic DcXyn30 catalyzed extraction process was optimized with respect to pH and temperature in a statistically designed experiment.

The highest yield based on the SEC peak area ranging from 5 – 110 kDa was obtained at pH 5.2 and 39°C (Figure 1A and B). When using the amount of reducing ends as the indicator, a similar pH optimum (pH 5.4), but a different temperature optimum of 48.6°C was found (Figure 1C and D). Based on the overlapping optimal areas using both quantification methods, the common optimal temperature was 45°C and optimal pH was 5.3. On this basis we opted to conduct extractions at 45 °C, pH 5.5. The combined pH-temperature optimum for DcXyn30 has not been reported previously, but an optimal pH of 5.5 has been used in previous studies of the enzyme.[26]

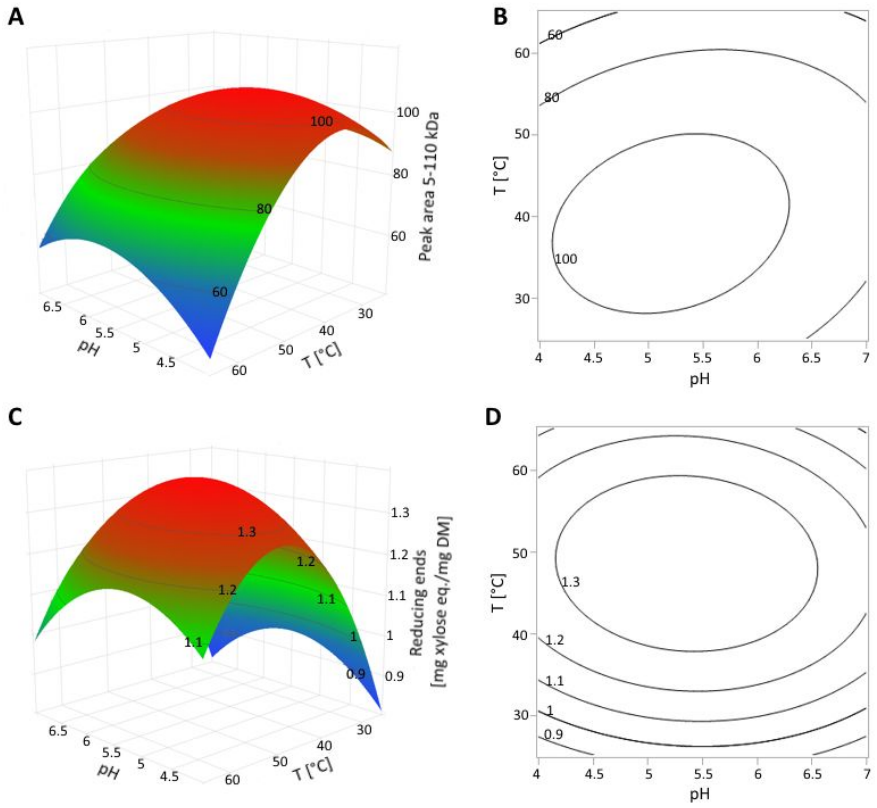

Figure 1: Enzymatic DcXyn30 extraction process optimization at different pH values (4.0, 5.5, 7.0) and temperatures (25, 45, 65°C). The reaction was carried out for 1 h in pH-adjusted dH_2O with 100 mg/ml destarched corn bran and 10 µg/ml purified DcXyn30. A) and B) Model based on peak area (5 – 110 kDa) from SEC analysis. C) and D) Model based on reducing end analysis.

A detailed analysis of the SEC analysis data obtained during longer enzymatic treatment (4 h) with DcXyn30 showed that the broad main peak gradually "moved" to the right with time, indicating that the average molecular weight of the extracted population of FGAX molecules decreased only slowly from ~41 kDa to ~10 kDa during extended DcXyn30 reaction (Figure 2).

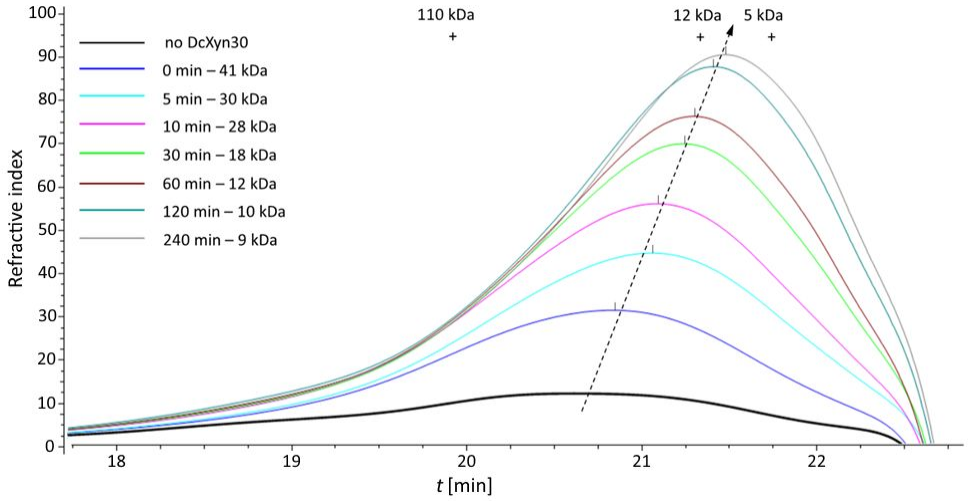

Figure 2: Time course of DcXyn30 catalyzed FGAX extraction from corn bran over 4 h: SEC for FGAX extracts (standards of 5, 12 and 110 kDa are indicated by +). The gradual decrease of the molecular weight at the peak maximum is indicated by a dashed arrow. The insert to the left lists the estimated average molecular weights of the extracted FGAX molecules at the different time points. The sample at 0 min was taken immediately after addition of enzyme.

The highest overall yield was achieved after 2 h of incubation with DcXyn30 (Figure 2). Further incubation did not lead to any significant increase in neither the peak area nor the quantified reducing ends (Figure S1). This congruence between the level of reducing ends and the total amount of the enzymatically extracted FGAX polysaccharides verify that the DcXyn30 had a very low preference for attacking the already released FGAX polysaccharides, supporting that DcXyn30 catalyzed the selective release of stable, high molecular weight FGAX molecules from corn bran. This result is explained by DcXyn30's well-defined recognition site for cleavage, which requires presence of a GlcA residue on the second xylosyl downstream the cleavage site. The data also support that the specific GlcA substitution pattern required for GH30_8 xylanase cleavage occurs quite rarely in corn bran arabinoxylan.[26,27]

The relative amount of such a recognition site can be calculated as follows: Assuming a theoretical xylan fragment of 110 kDa in the original corn bran, which was cut to fragments of 12 kDa after one hour (Figure 2), would mean that the original fragment was cleaved eight times, which corresponds to a relative amount of 1.4 mol-% of the recognition site for the GH30_8 xylanase.

Characterization of the extracted FGAX polymer. The yield of ethanol precipitated FGAX (3 % (w of FGAX/w of initial corn bran), 6% (w of arabinoxylan/w of initial arabinoxylan in corn bran)) obtained with the DcXyn30 treatment was higher, but comparable to previously reported data for mild alkaline arabinoxylan extraction from corn bran (typical yields of ~1.0 % (w/w)).[54] The monosaccharide composition and FA content of the ethanol precipitated DcXyn30 released FGAX was compared to the full DcXyn30 released FGAX extract (w/o precipitation) and to the destarched corn bran starting material. The monosaccharide and GlcA contents of the destarched corn bran (Table 1) were in good agreement with previously reported values on the same material,[45] but the observed relatively higher level of DiFAs as compared to FA levels contrasts previous findings (from our own lab).[45] We ascribe the latter difference to the use of more sensitive instrumentation in the present study, i.e. the LC-MS based quantitation versus the conventional reverse phase HPLC analyses that we employed previously.[45]

Detailed comparison of the composition of the full DcXyn30 released FGAX extract, the ethanol precipitated FGAX and the destarched corn bran starting material (Table 1) unveiled that arabinose, xylose and GlcA contents were richest in the FGAX extracts, underlining that the target FGAX polysaccharides were indeed extracted. The extracted FGAX polysaccharides were particularly enriched in arabinose and GlcA by a factor >2 compared to the starting material, and also rich in xylose and galacturonic acid (GalA) (1.1x and 1.4x compared to the corn bran)

(Table 1). As expected, almost no glucose was extracted. The composition of the DcXyn30 released FGAX extract and the ethanol-precipitated FGAX extract did not differ significantly. This verified that the raw extract indeed consisted mainly of the target FGAX polysaccharides.

The arabinose:xylose ratio of 1.18 of the ethanol-precipitated FGAX indicated an extremely high degree of doubly arabinose-substituted xylosyls. To estimate the amount of single and double arabinose-substitutions the following was considered: The composition analysis (Table 1) showed that 15.5 mol-% of the xylosyls were acetylated and 5.6 mol-% carried a GlcA moiety. The same amount (5.6 mol-%) was assumed for un-substituted xylose, because DcXyn30 requires an un-substituted xylosyl unit next to the GlcA as recognition site. The molar percentage of arabinose-decorated xylosyls in corn bran was then estimated as follows:

100% – 15.5% (acetylation) – 5.6% (Gal subst.) – 5.6% (GlcA subst.) – 5.6% (unsubst. xylose) = 67.7%

Hence, the amount of xylose carrying at least one arabinose-substitution is therefore estimated to be 203 g/kg DM (0.677·300 g/kg). Therefore, the percentage of arabinose moieties involved in double arabinose-substitutions on xylose in the ethanol precipitated DcXyn30 can be calculated to be: ((354 – 203)·100)/300 = 50.3%.

This estimate indicates that approx. 17% of the present xylosyl units carry a single arabinose and that approx. 50% of the present xylosyl moieties are decorated with two arabinoses.

The data (Table 1) and the xylan substitution estimations imply the following: a) that the DcXyn30 extracted FGAX is rich in esterified FAs that would be available for oxidative enzymatic cross-linking, and b) that a fraction of the extracted FGAX appear to be cross-linked already and is assumingly double-stranded FGAX (to be discussed further below).

Table 1. Monosaccharide composition of the destarched corn bran, raw extract and the ethanol precipitated DcXyn30 extracted FGAX.

Amount (g/kg DM)	Destarched corn bran	Full FGAX extract	Ethanol-precipitated FGAX extract
Arabinosyl	160 ± 2.7	350 ± 4.7	354 ± 5.0
Galactosyl	42.8 ± 0.8	16.8 ± 0.0	20.3 ± 0.0
Glucosyl	200 ± 5.1	10.3 ± 1.6	7.6 ± 0.0
Xylosyl	261 ± 4.5	311 ± 6.3	300 ± 7.4
Mannosyl	11.4 ± 0.6	2.24 ± 0.0	1.1 ± 0.2
Galacturonic Acid	10.4 ± 2.0	12.9 ± 0.7	14.9 ± 0.5
Glucuronic Acid	10.5 ± 0.2	21.1 ± 1.3	21.8 ± 0.3
Sugar total	696 ± 16	724 ± 15	720 ± 13
Ferulate	18.2 ± 0.8	16.8 ± 0.1	21.8 ± 0.2
Diferulate	23.0 ± 0.7	n.d.	12.0 ± 1.8
Acetyl	n.d.	n.d	18.6 ± 1.1
Lignin	7.0 ± 0.3	n.d	n.d
Loss (analytical loss)	255.3	n.d	314.0

n.d.: not determined; all values are averages of three independent experiments given ± s.d.

Whereas the FA content in the FGAX extract was similar to the level in the starting material, the content of diFAs in the precipitated FGAX extract was a factor of ~2 lower than that in the starting corn bran material. The latter result is not surprising as it is a generally accepted hypothesis that the presence of diFAs impedes enzymatic access to the xylan backbone as the diFAs cross-link the arabinoxylan chains and may be involved in xylan coupling to lignin.[55,56] Based on the FA and DiFA content of the enzymatically extracted FGAX, we estimate that 7.3 mol-% of all arabinoses in the FGAX carry a feruloyl (4.7 mol-%) or diferuloyl esterification (2·1.3 mol-%) as modification, which is in accord with previous data.[45] Additionally, the

arabinose in the extracted FGAX may be modified with another xylose residue or a xylose-galactose dimer via glycosidic linkages. However, from the available compositional data it is not possible to calculate the amount of arabinose side-chain modifications by glycosidic linkages.

A deeper assessment of the levels of the DiFAs in the DcXyn30 released ethanol-precipitated FGAX extract and the destarched corn bran showed that the relative levels of DiFAs were as expected, i.e. with highest abundancy of 8-O-4' DiFA.[57] However, the two most abundant DiFAs (5-5' and 8-O-4') were depleted by a factor >2 in the FGAX extract compared to the level in the starting material (Table 2), whereas the level of the other DiFAs in the FGAX extract was almost similar to the level found in the original destarched corn bran (Table 2).

Table 2. Ferulic acid (FA) and diferulic acid (DiFA) content of the destarched corn bran, and the ethanol precipitated FGAX extract.

Amount (g/kg DM)	Destarched corn bran	Ethanol-precipitated FGAX extract*
Ferulate	18.2 ± 0.8	21.2 ± 0.2
8-8' aryl DiFA	4.04 ± 0.31	3.64 ± 0.34
8-8' DiFA	0.14 ± 0.02	0.38 ± 0.07
8-5' DiFA	1.04 ± 0.03	1.24 ± 0.35
5-5' DiFA	4.90 ± 0.10	1.38 ± 0.43
8-O-4' DiFA	10.6 ± 0.1	4.09 ± 0.25
8-5' benzo DiFA	2.75 ± 0.08	1.23 ± 0.36

n.d.: not determined; values represent the average and standard deviation of three independent experiments. *DiFA levels in the full extract were below the detection limit.

The depletion of the 8-O-4' DiFA might be due to its higher vulnerability to cleavage compared to the other DiFAs. Based on this finding, we further speculate that the 8-8' aryl DiFA might be an exclusive feature of the extracted FGAX, which is found in lower amounts in other

parts of the corn bran xylan and/or cell wall components (only trace amounts of triferulic acids were detected and not included in the quantifications).

The NMR spectrum of the precipitated FGAX affirmed the presence of glucurono-arabino-xylan (Figure 3A). Detailed analysis of the arabinofuranosyl signals (Figure 3B and Figure S2) confirmed the high degree of arabinose double-substitutions. Also, presence of (low amounts of) arabinose-xylose side-chains was confirmed. To assess the calculations based on the composition data, a semi-quantitative analysis of the 2D-NMR data was carried out. Analysis of the spectra before and after sample saponification (Figure S3) revealed that 19 mol-% of the xylose was acetylated, which is in agreement with the 15.5 mol-% estimated above. The NMR data also supported an arabinose feruloylation/diferuloylation degree of 7.3 mol-% with an estimated feruloylation degree of 10 mol-%. Furthermore, the NMR data suggested a molar ratio of arabinose:xylose:uronic acids of 8.6:6.3:1 (spectral regions for GlcA and GalA overlapped in the FGAX NMR spectra). The ratio of double:single arabinose substitutions on the backbone as determined by NMR supported the ratio of 2.9:1. The high arabinose:xylose ratio led us to re-investigate presence of other sources for arabinose than arabinoxylan. Comparison of the 2D-NMR spectra of the precipitated FGAX with linear 1,5-α-L-arabinan (Figure 3C) indeed showed presence of 1,5-α-L-arabinan. It cannot be definitively concluded that the dimeric (or any oligomeric) 1,5-α-L-arabinan is not originating from low levels of pectin in the FGAX extract. However, oligomeric arabinofuranosyl sidechains have previously been reported on xylan isolated from corn kernels[6,7] as well as from sorghum[58] and bark of cinnamon trees based on linkage analysis data.[59] The NMR data here (Figure 3) are the first spectroscopic evidence of arabinan-like side-chains in FGAX from corn bran. Only for sorghum glucuronoarabinoxylan presence of oligomeric arabinosyl sidechains has previously been shown by NMR.[58]

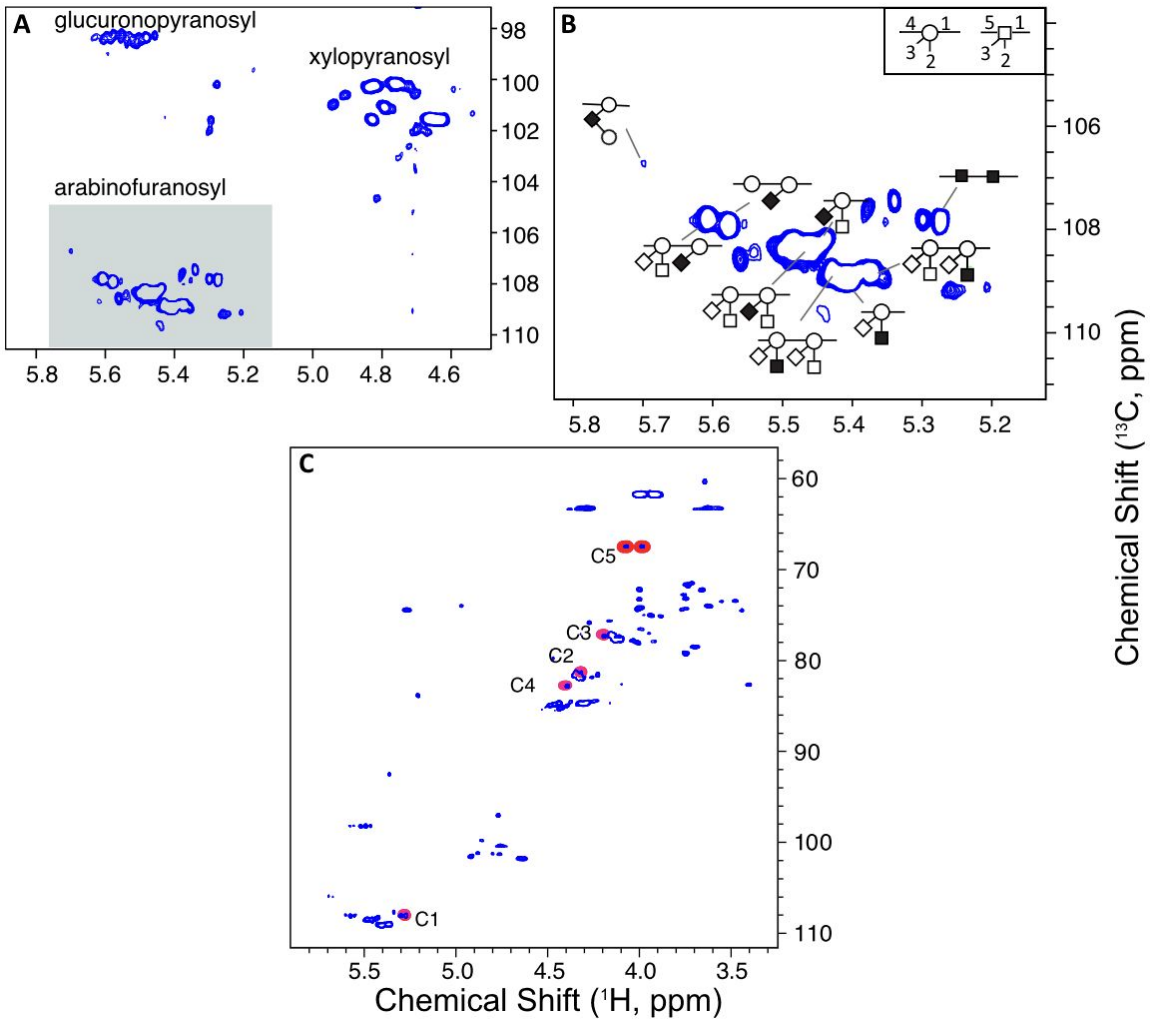

Figure 3: ^{1}H-^{13}C HSQC NMR spectra of the FGAX extract. A) 2D spectrum highlighting the glucuronopyranosyl, xylopyranosyl and arabinofuranosyl signals. B) Zoom into the arabinofuranosyl area highlighted as a grey box in A). Xylose units are shown as circles and arabinoses as squares. The glycosidic bonds are shown as schematically depicted in the upper right corner of B). The residue responsible for a specific anomeric signal is highlighted in black. C) Overlayed 2D spectra of precipitated extracted FGAX (blue signals) and of pure 1,5-arabinan (red signals). The carbon atoms of arabinose residues in the pure arabinan were assigned to specific signals by the use of heteronuclear assignment spectra (Figure S2) and validated by comparison to literature assignments.[60]

Substitution pattern of the GH30_8 recognition site in FGAX. We wanted to obtain more insight into the substitution pattern close to the recognition site of the GH30_8 enzymes including a GlcA residue. The available crystal structure of DcXyn30[27] was therefore investigated and two substrate analogues were docked into the active site (Figure 4A and B).

This docking revealed that the xylosyl in subsite +1 can carry substitutions on either O2 and/or O3. Even an arabinosyl residue in both positions would be possible based on the available cavity volume in the enzyme. Decorations on the xylosyl in subsite -3 appear slightly more restricted. The enzyme can apparently not accommodate an arabinosyl in position O2, but an acetyl residue in that position as well as any substituent (arabinosyl or acetyl) on O3 would be possible. Such an arabinosyl residue in proximity to a GlcA was described for xylan from corn stover, so a substitution in this position seems plausible.[61] This finding could also explain the recalcitrance of corn GAX towards degradation by xylanases from family GH10, which were shown to cleave the xylan backbone in between an unsubstituted xylosyl and a GlcA-decorated xylosyl residue.[62]

The presence of an acetyl residue on O3 of the same xylosyl carrying the GlcA was described also,[61] which seems plausible with respect to space requirements in the active site of DcXyn30. An arabinosyl residue in that position is, however, too big to be accommodated by the enzyme.

The most restricted xylosyl residue in terms of substitutions is the xylosyl in subsite -1. The O3 of this residue has to be unsubstituted, because binding in the very narrow cleft (Figure 4A) close to the catalytic amino acid (E165) would otherwise not be possible. However, we found a small tunnel in the structure just next to E165, which hosted three water molecules in the structure.[27] Docking of an acetyl modified substrate analogue revealed that such an acetyl would fit perfectly into this tunnel upon binding (Figure 4B).

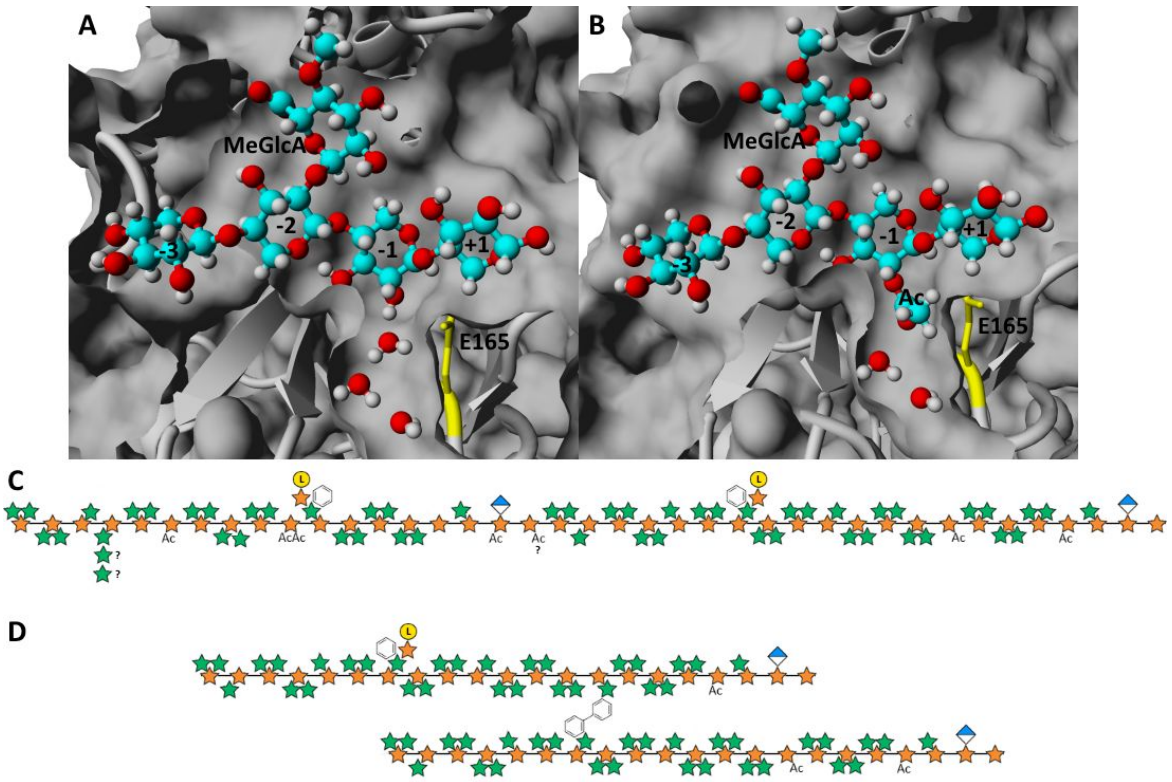

Figure 4: A and B: Active site 3D model representation of DcXyn30 with a substrate molecule docked. The enzyme and its surface are shown in grey, the catalytic residue (E165) is highlighted in yellow. The docked substrate and specific water molecules in the structure are shown as ball-and-stick models with hydrogen atoms in white, carbon atoms in cyan and oxygen atoms in red. The substrate binding sites and the cleavage site are indicated by the numbers -3 to +1 (the substrate is cleaved between -1 and +1). A: The substrate used for docking was 2^3-(4-*O*-methyl-α-D-glucuronyl)-xylotetraose, B: The substrate used for docking was 2^2-(acetyl)-2^3-(4-*O*-methyl-α-D-glucuronyl)-xylotetraose. C and D: Stylized structures of 16 kDa FGAX fragments based on our interpretation of the data. Orange stars: xylosyl, green stars: arabinosyl, blue/white diamond: GluA, yellow circle: galactose (L indicates L-galactose), phenol ring: feruloyl residue, two connected phenol rings: diferuloyl cross-link, Ac: acetyl residue. Positions of the substituents (above or below) on the xylan backbone do not reflect actual bonds to specific carbon atoms.

Due to the significant amounts of DiFAs in the enzymatically extracted FGAX we speculate that it must contain a certain number of fragments that are already cross-linked, and we thus presume that the DcXyn30 catalysis release both single-stranded and double-stranded FGAX molecules, where the double-stranded molecules are DiFA-cross-linked (Figure 4D).

FGAX-based hydrogel formation. Oxidative gelation of 2% FGAX solutions by enzymatic cross-linking was catalyzed by laccases from *Myceliophthora thermophila* (MtL) and *Pleurotus ostreatus* (PoL) which were dosed according their activity on syringaldazine (equivalent activity at pH 5.0). The development of storage (G') and loss (G'') moduli during the cross-linking was studied over time (Figure 5A). Both laccases catalyzed oxidative cross-linking that resulted in gel formation as evident from the increase of G' according to a regular hyperbola curve. The G' of FGAX solutions, in which oxidative cross-linking was catalyzed by MtL increased with time almost instantaneously after start of the reaction (after 2 min.). The initial rate of gelation was determined from the initial slope of G' as a function of time for G' > G'', yielding an average gelation rate of 0.47±0.06 Pa min^{-1}. In contrast, FGAX solutions in which oxidative cross-linking was catalyzed by PoL showed a lag-phase of ~25 min (Figure 5A) before the G' started to increase with an average gelation rate of 0.27±0.06 Pa min^{-1}. The lag-phase and lower gelation rate achieved with PoL catalysis suggest that MtL catalyzed oxidation of the feruloyls faster than PoL. Apparently, a threshold concentration of DiFA had to be obtained before gel formation was reflected in the rheological measurements; hence, from the analogous chemical analyses of the laccase catalyzed formation of DiFA and depletion of FA (Figure 5B), it was evident that the formation of DiFA also occured at a higher rate with MtL than with PoL catalysis. MtL catalysis thus resulted in a DiFA concentration of 1.8 mM after 5 min, whereas it took more than 20 min to reach a DiFA level above 1.5 mM with the PoL (Figure 5B).

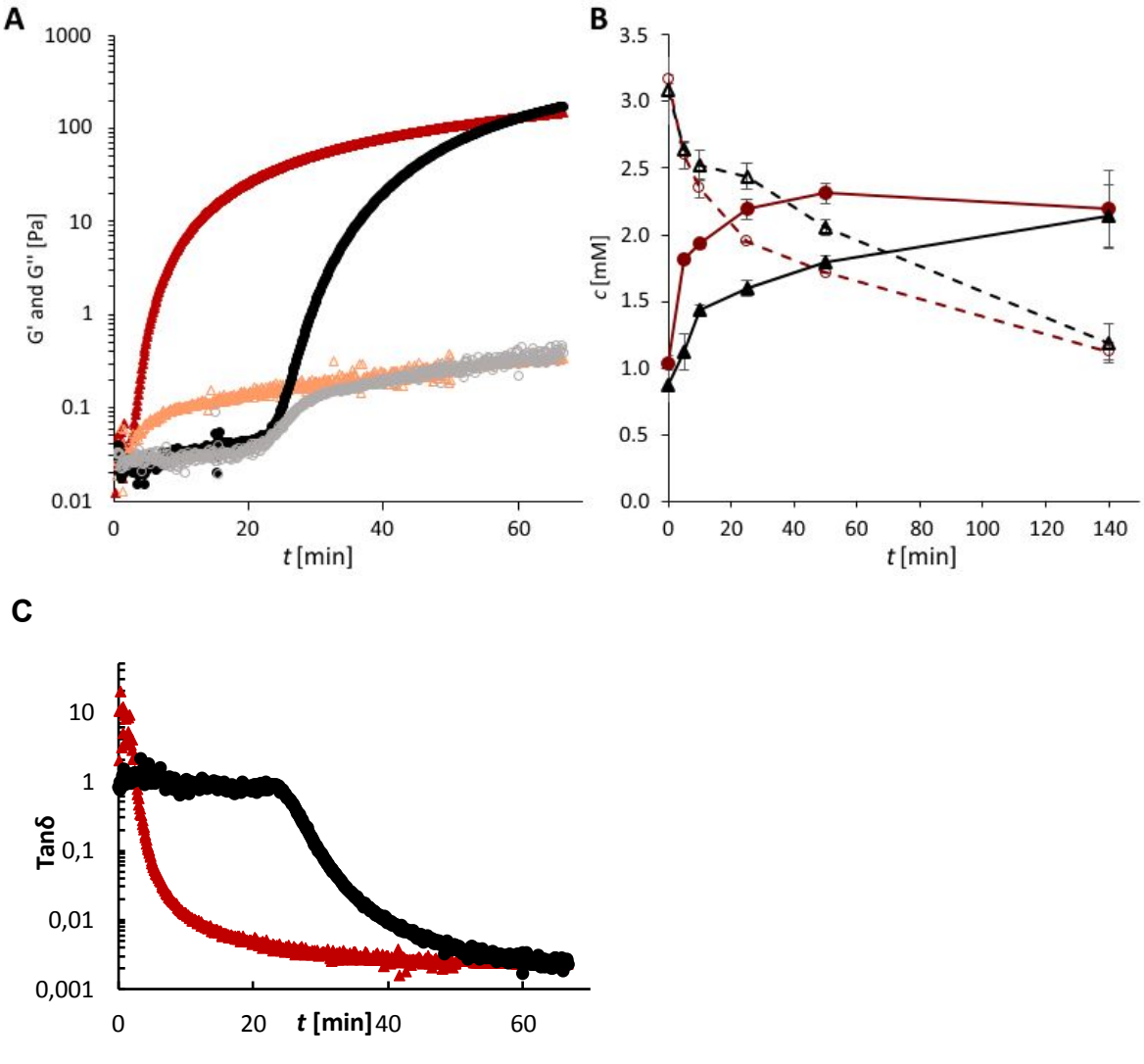

Figure 5: A) Progress in hydrogel formation of DcXyn30 extracted FGAX over time during enzymatic catalysis with MtL (red and orange triangles) and PoL (black and grey circles), respectively, measured as increase in elastic modulus (G', red and black closed symbols) and viscous modulus (G'', orange and grey open symbols). B) Formation of diferulic acids (DiFAs, closed symbols) and loss in ferulic acid (FA, open symbols) concentration in DcXyn30 extracted FGAX over time during MtL (red circles) and PoL (black triangles) catalytic treatment. C) Progress in the loss factor tan δ (G''/G') with time during laccase catalyzed hydrogel formation of DcXyn30 extracted FGAX with MtL (red) and PoL (black), respectively.

The evolution of the elastic behavior plotted at the progress in the loss factor tan δ with time (Figure 5C) further verified that the phase transition from solution to gel happened rapidly and continuously with MtL catalysis, whereas gel formation only started after ca. 25 min with the PoL treatment. However, after 60 min (at the end of the treatment) the tan δ values for the gels formed by the two different laccase treatments were similar (Figure 5C). Together with the gelation kinetics assessed from the progress in elastic modulus (G') and viscous modulus (G'') (Figure 5A) and the chemical data (Figure 5B), the data corroborate that the reaction first involves a rapid formation of covalent bonds between the FA moieties of neighboring chains of FGAX; and then progresses to produce a cross-linked polymer network; further the network obtained with either laccase appeared to display similar gel properties after extended reaction.

The cross-linking experiments were accomplished with the FGAX solution at pH 6.5. Control assays at pH 6.5 (with syringaldazine) verified that the activities of the MtL were similar at pH 5.0 and 6.5; whereas the PoL activity at pH 6.5 (in the syringaldazine assay) was only ~25% of the activity at pH 5.0. The data are in accord with the reported pH optima for PoL, which are typically in the range of pH 3 – 5,[63,64] whereas for MtL a slightly higher pH optimum range of pH 5.8-6.5 has been reported.[65–67] We therefore ascribe the differences in the laccase catalyzed cross-linking rates, and hence the lag-phase of the PoL reaction, to differences in pH optima for the two laccases.

Conclusions

The enzymatically extracted FGAX molecules turned out to contain diferulates in addition to single feruloyl-substitutions leading us to interpret that the DcXyn30 catalysis on corn bran released both single and double-stranded FGAX polysaccharides. Due to the distinct catalytic selectivity of the DcXyn30, requiring a glucuronosyl (GlcA) or 4-O-methyl-GlcA residue as recognition site for cleavage[24], the solubilized FGAX molecules were essentially stable in solution even during prolonged enzymatic treatment with DcXyn30. In addition to confirming a high extent of doubly substituted xylosyl moieties having arabinosyl substitutions on both O2 and O3, NMR analysis also revealed the presence of dimeric (or oligomeric) 1,5-α-L-arabinan in the extracted corn bran FGAX. Although the possibility that these 1,5-α-L-arabinan dimers originate from pectin cannot be firmly excluded (low levels of pectin may be present in raw corn bran), we consider it likely that these arabinan dimers are substitutions on the FGAX xylan. Oligomeric arabinan sidechains have been reported on xylan from corn kernels[6,7], sorghum[58], and from cinnamon tree bark[59], but the possible existence of such substitutions in corn bran glucurono-arabinoxylan is a novel finding. Laccase catalyzed covalent cross-linking of the feruloyl-groups to form DiFAs in the solubilized FGAX polysaccharides resulted in formation of firm hydrogels. Rheological monitoring of the gel formation progress of the cross-linking reactions showed that *M. thermophila* laccase catalyzed cross-linking was faster than the *P. ostreatus* laccase, but the gels obtained had similar hardness and elasticity properties. We ascribe the difference in cross-linking rate to activity differences of the two laccases at the cross-linking pH of 6.5. The data present a new enzymatic approach using a highly selective GH30 xylanase to catalyze release of long-chain FGAX from corn bran, and display functional utilization of FGAX from corn bran, which could pave the way for novel bioeconomy valorization uses of corn bran.

Supporting Information

The Supporting Information includes 3 Figures: Progress of DcXyn30 catalyzed FGAX extraction; HSQC and HMBC spectra for 1,5-arabinan; overlayed 2D spectra of precipitated FGAX and saponified FGAX.

Conflict of interest

The authors declare no competing financial interests.

Author Contributions

ASM, PU, JM and LM perceived the study. JM did cloning, expression, and molecular docking of DcXyn30. ML and LM analyzed corn bran, LM and KL optimized DcXyn30 extraction, SM performed the NMR work and NMR data analysis, LM and AP did cross-linking and rheology, and LM did all LC-MS analyses. The manuscript was written by LM, JM, and ASM with contributions from all co-authors. All authors have approved the final version of the manuscript.

Funding Sources

This research was supported by the Innovation Fund Denmark (Project No. 5152-00001B). The 800 MHz NMR spectra were acquired on instruments of the NMR center DTU funded by the Villum Foundation.

Acknowledgment

We thank Novozymes (Bagsværd, Denmark) for donating the *M. thermophila* laccase and Professor Maher Abou Hachem, DTU Bioengineering, for the 1,5-α-L-arabinan sample.

ABBREVIATIONS

FGAX, glucuronoarabinoxylan; GH, glycoside hydrolase; DcXyn30, GH30_8 xylanase from *Dickeya chrysanthemi*; GlcA, glucuronic acid; DM, dry matter; FA, ferulic acid; DiFA, diferulic

acid; GalA, galacturonic acid; Gal, galactose; Ara, arabinose; Glc, glucose; Xyl, xylose; Man, mannose; MtL, laccase from *Myceliophtora thermophila*; PoL, laccase from *Pleurotus ostreatus*.

REFERENCES

(1) Mahapatra, A.; Lan, Y. Postharvest Handling of Grains and Pulses. In *Handbook of Food Preservation*; Rahman, M. S., Ed.; CRC Press, 1999; pp 74–129.

(2) United States Department of Agriculture: Foreign Agricultural Service. *Grain: World Markets and Trade*; 2019.

(3) Rose, D. J.; Inglett, G. E.; Liu, S. X. Utilisation of Corn (*Zea mays*) Bran and Corn Fiber in the Production of Food Components. *J. Sci. Food Agric.* **2010**, *90* (6), 915–924. https://doi.org/10.1002/jsfa.3915.

(4) Saulnier, L.; Marot, C.; Chanliaud, E.; Thibault, J. F. Cell Wall Polysaccharide Interactions in Maize Bran. *Carbohydr. Polym.* **1995**, *26* (4), 279–287. https://doi.org/10.1016/0144-8617(95)00020-8.

(5) Appeldoorn, M. M.; de Waard, P.; Kabel, M. A.; Gruppen, H.; Schols, H. A. Enzyme Resistant Feruloylated Xylooligomer Analogues from Thermochemically Treated Corn Fiber Contain Large Side Chains, Ethyl Glycosides and Novel Sites of Acetylation. *Carbohydr. Res.* **2013**, *381*, 33–42. https://doi.org/10.1021/jf102849x.

(6) Huisman, M. M.; Schols, H.; Voragen, A. G. Glucuronoarabinoxylans from Maize Kernel Cell Walls Are More Complex than Those from Sorghum Kernel Cell Walls. *Carbohydr. Polym.* **2000**, *43* (3), 269–279. https://doi.org/10.1016/S0144-8617(00)00154-5.

(7) Nishitani, K.; Nevins, D. J. Enzymic Analysis of Feruloylated Arabinoxylans (Feraxan)

Derived from *Zea mays* Cell Walls. *Plant Physiol.* **1989**, *91*, 242–248. https://doi.org/10.1104/pp.93.2.396.

(8) Appeldoorn, M. M.; Kabel, M. A.; Van Eylen, D.; Gruppen, H.; Schols, H. A. Characterization of Oligomeric Xylan Structures from Corn Fiber Resistant to Pretreatment and Simultaneous Saccharification and Fermentation. *J. Agric. Food Chem.* **2010**, *58* (21), 11294–11301. https://doi.org/10.1021/jf102849x.

(9) Allerdings, E.; Ralph, J.; Steinhart, H.; Bunzel, M. Isolation and Structural Identification of Complex Feruloylated Heteroxylan Side-Chains from Maize Bran. *Phytochemistry* **2006**, *67* (12), 1276–1286. https://doi.org/10.1016/j.phytochem.2006.04.018.

(10) Selig, M. J.; Adney, W. S.; Himmel, M. E.; Decker, S. R. The Impact of Cell Wall Acetylation on Corn Stover Hydrolysis by Cellulolytic and Xylanolytic Enzymes. *Cellulose* **2009**, *16* (4), 711–722. https://doi.org/10.1007/s10570-009-9322-0.

(11) Biely, P. Microbial Carbohydrate Esterases Deacetylating Plant Polysaccharides. *Biotechnol. Adv.* **2012**, *30* (6), 1575–1588. https://doi.org/10.1016/j.biotechadv.2012.04.010.

(12) Schendel, R. R.; Meyer, M. R.; Bunzel, M. Quantitative Profiling of Feruloylated Arabinoxylan Side-Chains from Graminaceous Cell Walls. *Front. Plant Sci.* **2016**, *6*, 1249. https://doi.org/10.3389/fpls.2015.01249.

(13) Nordberg Karlsson, E.; Schmitz, E.; Linares-Pastén, J. A.; Adlercreutz, P. Endo-Xylanases as Tools for Production of Substituted Xylooligosaccharides with Prebiotic Properties. *Appl. Microbiol. Biotechnol.* **2018**, 9081–9088.

https://doi.org/10.1007/s00253-018-9343-4.

(14) Falck, P.; Linares-Pastén, J. A.; Karlsson, E. N.; Adlercreutz, P. Arabinoxylanase from Glycoside Hydrolase Family 5 Is a Selective Enzyme for Production of Specific Arabinoxylooligosaccharides. *Food Chem.* **2018**, *242*, 579–584. https://doi.org/10.1016/j.foodchem.2017.09.048.

(15) Niño-Medina, G.; Carvajal-Millan, E.; Rascon-Chu, A.; Marquez-Escalante, J. A.; Guerrero, V.; Salas-Muñoz, E. Feruloylated Arabinoxylans and Arabinoxylan Gels: Structure, Sources and Applications. *Phytochem. Rev.* **2010**, *9* (1), 111–120. https://doi.org/10.1007/s11101-009-9147-3.

(16) Zhang, X.; Chen, T.; Lim, J.; Gu, F.; Fang, F.; Cheng, L.; Campanella, O. H.; Hamaker, B. R. Acid Gelation of Soluble Laccase-Crosslinked Corn Bran Arabinoxylan and Possible Gel Formation Mechanism. *Food Hydrocoll.* **2019**, *92*, 1–9. https://doi.org/10.1016/j.foodhyd.2019.01.032.

(17) Carvajal-Millan, E.; Landillon, V.; Morel, M.-H.; Rouau, X.; Doublier, J.-L.; Micard, V. Arabinoxylan Gels: Impact of the Feruloylation Degree on Their Structure and Properties. *Biomacromolecules* **2005**, *6* (1), 309–317. https://doi.org/10.1021/bm049629a.

(18) Rose, D. J.; Inglett, G. E. Production of Feruloylated Arabinoxylo-Oligosaccharides from Maize (*Zea mays*) Bran by Microwave-Assisted Autohydrolysis. *Food Chem.* **2010**, *119* (4), 1613–1618. https://doi.org/10.1016/j.foodchem.2009.09.053

(19) Ruthes, A. C.; Martínez-Abad, A.; Tan, H.-T.; Bulone, V.; Vilaplana, F. Sequential Fractionation of Feruloylated Hemicelluloses and Oligosaccharides from Wheat Bran

Using Subcritical Water and Xylanolytic Enzymes. *Green Chem.* **2017**, *19* (8), 1919–1931. https://doi.org/10.1039/c6gc03473j

(20) Rudjito, R. C.; Ruthes, A. C.; Jiménez-Quero, A.; Vilaplana, F. Feruloylated Arabinoxylans from Wheat Bran: Optimization of Extraction Process and Validation at Pilot Scale. *ACS Sustain. Chem. Eng.* **2019**, *7* (15), 13167–13177. https://doi.org/10.1021/acssuschemeng.9b02329.

(21) Rasmussen, L. E.; Sørensen, J. F.; Meyer, A. S. Kinetics and Substrate Selectivity of a *Triticum aestivum* Xylanase Inhibitor (TAXI) Resistant D11F/R122D Variant of *Bacillus subtilis* XynA Xylanase. *J. Biotechnol.* **2010**, *146* (4), 207–214. https://doi.org/10.1016/j.jbiotec.2010.02.012.

(22) Gao, D.; Uppugundla, N.; Chundawat, S. P.; Yu, X.; Hermanson, S.; Gowda, K.; Brumm, P.; Mead, D.; Balan, V.; Dale, B. E. Hemicellulases and Auxiliary Enzymes for Improved Conversion of Lignocellulosic Biomass to Monosaccharides. *Biotechnol. Biofuels* **2011**, *4*, 5. https://doi.org/10.1186/1754-6834-4-5

(23) Rose, D. J.; Inglett, G. E. A Method for the Determination of Soluble Arabinoxylan Released from Insoluble Substrates by Xylanases. *Food Anal. Methods* **2011**, *4* (1), 66–72. https://doi.org/10.1007/s12161-009-9121-0.

(24) Biely, P.; Singh, S.; Puchart, V. Towards Enzymatic Breakdown of Complex Plant Xylan Structures: State of the Art. *Biotechnol. Adv.* **2016**, *34* (7), 1260–1274. https://doi.org/10.1016/j.biotechadv.2016.09.001.

(25) Nishitani, K.; Nevins, D. J. Glucuronoxylan Xylanohydrolase: A Unique Xylanase with Requirement for Appendant Glucuronosyl Units. *J. Biol. Chem.* **1991**, *266*, 6539-6543.

(26) Vršanská, M.; Kolenová, K.; Puchart, V.; Biely, P. Mode of Action of Glycoside Hydrolase Family 5 Glucuronoxylan Xylanohydrolase from *Erwinia chrysanthemi*. *FEBS J.* **2007**, *274* (7), 1666–1677. https://doi.org/10.1111/j.1742-4658.2007.05710.x.

(27) Urbániková, L.; Vršanská, M.; Mørkeberg Krogh, K. B. R.; Hoff, T.; Biely, P. Structural Basis for Substrate Recognition by *Erwinia chrysanthemi* GH30 Glucuronoxylanase. *FEBS J.* **2011**, *278* (12), 2105–2116. https://doi.org/10.1111/j.1742-4658.2011.08127.x.

(28) Gallardo, Ó.; Fernández-Fernández, M.; Valls, C.; Valenzuela, S. V.; Blanca Roncero, M.; Vidal, T.; Díaz, P.; Javier Pastor, F. I. Characterization of a Family GH5 Xylanase with Activity on Neutral Oligosaccharides and Evaluation as a Pulp Bleaching Aid. *Appl. Environ. Microbiol.* **2010**, *76* (18), 6290–6294. https://doi.org/10.1128/AEM.00871-10.

(29) St. John, F. J.; Rice, J. D.; Preston, J. F. Characterization of XynC from *Bacillus subtilis* subsp. *subtilis* Strain 168 and Analysis of Its Role in Depolymerization of Glucuronoxylan. *J. Bacteriol.* **2006**, *188* (24), 8617–8626. https://doi.org/10.1128/JB.01283-06.

(30) Sakka, M.; Tachino, S.; Katsuzaki, H.; van Dyk, J. S.; Pletschke, B. I.; Kimura, T.; Sakka, K. Characterization of Xyn30A and Axh43A of *Bacillus licheniformis* SVD1 Identified by Its Genomic Analysis. *Enzyme Microb. Technol.* **2012**, *51* (4), 193–199. https://doi.org/10.1016/j.enzmictec.2012.06.003.

(31) St. John, F. J.; Dietrich, D.; Crooks, C.; Balogun, P.; de Serrano, V.; Pozharski, E.; Smith,

J. K.; Bales, E.; Hurlbert, J. A Plasmid Borne, Functionally Novel Glycoside Hydrolase Family 30 Subfamily 8 Endoxylanase from Solventogenic *Clostridium*. *Biochem. J.* **2018**, *475* (9), 1533–1551. https://doi.org/10.1042/BCJ20180050.x

(32) St. John, F. J.; Dietrich, D.; Crooks, C.; Pozharski, E.; González, J. M.; Bales, E.; Smith, K.; Hurlbert, J. C. A Novel Member of Glycoside Hydrolase Family 30 Subfamily 8 with Altered Substrate Specificity. *Acta Crystallogr. Sect. D Biol. Crystallogr.* **2014**, *70* (11), 2950–2958. https://doi.org/10.1107/S1399004714019531.

(33) Maehara, T.; Yagi, H.; Sato, T.; Ohnishi-Kameyama, M.; Fujimoto, Z.; Kamino, K.; Kitamura, Y.; St. John, F. J.; Yaoi, K.; Kaneko, S. GH30 Glucuronoxylan-Specific Xylanase from *Streptomyces turgidiscabies* C56. *Appl. Environ. Microbiol.* **2018**, *84* (4), e01850-17. https://doi.org/10.1128/AEM.01850-17.

(34) Nakamichi, Y.; Fouquet, T.; Ito, S.; Watanabe, M.; Matsushika, A.; Inoue, H. Structural and Functional Characterization of a Bifunctional GH30-7 Xylanase B from the Filamentous Fungus *Talaromyces cellulolyticus*. *J. Biol. Chem.* **2019**, *294* (11), 4065–4078. https://doi.org/10.1074/jbc.ra118.007207.

(35) Katsimpouras, C.; Dedes, G.; Thomaidis, N. S.; Topakas, E. A Novel Fungal GH30 Xylanase with Xylobiohydrolase Auxiliary Activity. *Biotechnol. Biofuels* **2019**, *12*, 120. https://doi.org/10.1186/s13068-019-1455-2.

(36) Biely, P.; Puchart, V.; Stringer, M. A.; Mørkeberg Krogh, K. B. R. *Trichoderma reesei* XYN VI - A Novel Appendage-Dependent Eukaryotic Glucuronoxylan Hydrolase. *FEBS J.* **2014**, *281* (17), 3894–3903. https://doi.org/10.1111/febs.12925.

(37) Šuchová, K.; Kozmon, S.; Puchart, V.; Malovíková, A.; Hoff, T.; Mørkeberg Krogh, K. B. R.; Biely, P. Glucuronoxylan Recognition by GH 30 Xylanases: A Study with Enzyme and Substrate Variants. *Arch. Biochem. Biophys.* **2018**, *643*, 42–49. https://doi.org/10.1016/j.abb.2018.02.014.

(38) Puchart, V.; Mørkeberg Krogh, K. B. R.; Biely, P. Glucuronoxylan 3-O-Acetylated on Uronic Acid-Substituted Xylopyranosyl Residues and Its Hydrolysis by GH10, GH11 and GH30 Endoxylanases. *Carbohydr. Polym.* **2019**, *205*, 217–224. https://doi.org/10.1016/j.carbpol.2018.10.043.

(39) Biely, P.; Malovíková, A.; Hirsch, J.; Morkeberg Krogh, K. B. R.; Ebringerová, A. The Role of the Glucuronoxylan Carboxyl Groups in the Action of Endoxylanases of Three Glycoside Hydrolase Families: A Study with Two Substrate Mutants. *Biochim. Biophys. Acta - Gen. Subj.* **2015**, *1850* (11), 2246–2255. https://doi.org/10.1016/j.bbagen.2015.07.003.

(40) Keen, N. T.; Boyd, C.; Henrissat, B. Cloning and Characterization of a Xylanase Gene from Corn Strains of *Erwinia chrysanthemi*. *Mol. Plant-Microbe Interact.* **1996**, *9* (7), 651–657. https://doi.org/10.1094/MPMI-9-0651.

(41) Bertani, I.; Passos da Silva, D.; Abbruscato, P.; Piffanelli, P.; Venturi, V. Draft Genome Sequence of the Plant Pathogen *Dickeya zeae* DZ2Q, Isolated from Rice in Italy. *Genome Announc.* **2013**, *1* (6), e00905–e00913. https://doi.org/10.1128/genomeA.00905-13.

(42) Kumar, A.; Hunjan, M. S.; Kaur, H.; Rawal, R.; Kumar, A.; Singh. P. P. A Review on Bacterial Stalk Rot Disease of Maize Caused by *Dickeya zeae*. *J. Appl. Nat. Sci.* **2017**, *9* (2), 1214–1225. https://doi.org/10.31018/jans.v9i2.1348.

(43) Zhou, J.; Cheng, Y.; Lv, M.; Liao, L.; Chen, Y.; Gu, Y.; Liu, S.; Jiang, Z.; Xiong, Y.; Zhang, L. The Complete Genome Sequence of *Dickeya zeae* EC1 Reveals Substantial Divergence from Other *Dickeya* Strains and Species. *BMC Genomics* **2015**, *16*, 571. https://doi.org/10.1186/s12864-015-1545-x.

(44) Graham, D. C.; Dowson, W. J. The Coliform Bacteria Associated With Potato Black-Leg And Other Soft Rots. *Ann. Appl. Biol.* **1960**, *48* (1), 51–57. https://doi.org/10.1111/j.1744-7348.1960.tb03503.x.

(45) Agger, J. W.; Viksø-Nielsen, A.; Meyer, A. S. Enzymatic Xylose Release from Pretreated Corn Bran Arabinoxylan: Differential Effects of Deacetylation and Deferuloylation on Insoluble and Soluble Substrate Fractions. *J. Agric. Food Chem.* **2010**, *58* (10), 6141–6148. https://doi.org/10.1021/jf100633f.

(46) Sluiter, A.; Hames, B.; Ruiz, R.; Scarlata, C.; Sluiter, J.; Templeton, D.; Crocker, D. Determination of Structural Carbohydrates and Lignin in Biomass. Laboratory Analytical Procedure (LAP); NREL/TP-510-42618, Golden, CO, 2008.

(47) Petersen, T. N.; Brunak, S.; von Heijne, G.; Nielsen, H. SignalP 4.0: Discriminating Signal Peptides from Transmembrane Regions. *Nat. Methods* **2011**, *8* (10), 785–786. https://doi.org/10.1038/nmeth.1701.

(48) Waldron, K. W.; Parr, A. J.; Ng, A.; Ralph, J. Cell Wall Esterified Phenolic Dimers: Identification and Quantification by Reverse Phase High Performance Liquid Chromatography and Diode Array Detection. *Phytochem. Anal.* **1996**, *7* (6), 305–312. https://doi.org/10.1002/(SICI)1099-1565(199611)7:6<305::AID-PCA320>3.0.CO;2-A.

(49) Dobberstein, D.; Bunzel, M. Separation and Detection of Cell Wall-Bound Ferulic Acid Dehydrodimers and Dehydrotrimers in Cereals and Other Plant Materials by Reversed Phase High-Performance Liquid Chromatography with Ultraviolet Detection. *J. Agric. Food Chem.* **2010**, *58* (16), 8927–8935. https://doi.org/10.1021/jf101514j.

(50) Andreasen, M. F.; Christensen, L. P.; Meyer, A. S.; Hansen, Å. Ferulic Acid Dehydrodimers in Rye (*Secale cereale* L.). *J. Cereal Sci.* **2000**, *31*, 303–307. https://doi.org/10.1006/jcrs.1999.0296.

(51) Gruppen, H.; Hoffmann, R. A.; Kormelink, F. J. M.; Voragen, A. G. J.; Kamerlin, J. P.; Vliegenthart, J. F. G. Characterisation by ^{1}H NMR Spectroscopy of Enzymically Derived Oligosaccharides from Alkali-Extractable Wheat-Flour Arabinoxylan. *Carbohydr. Res.* **1992**, *233*, 45–64. https://doi.org/10.1016/S0008-6215(00)90919-4.

(52) Petersen, B. O.; Lok, F.; Meier, S. Probing the Structural Details of Xylan Degradation by Real-Time NMR Spectroscopy. *Carbohydr. Polym.* **2014**, *112*, 587–594. https://doi.org/10.1016/j.carbpol.2014.06.049.

(53) Krieger, E.; Vriend, G. YASARA View—Molecular Graphics for All Devices—from Smartphones to Workstations. *Bioinformatics* **2014**, *30* (20), 2981–2982. https://doi.org/10.1093/bioinformatics/btu426.

(54) Morales-Burgos, A. M.; Carvajal-Millan, E.; López-Franco, Y. L.; Rascón-Chu, A.; Lizardi-Mendoza, J.; Sotelo-Cruz, N.; Brown-Bojórquez, F.; Burgara-Estrella, A.; Pedroza-Montero, M. Syneresis in Gels of Highly Ferulated Arabinoxylans:

Characterization of Covalent Cross-Linking, Rheology, and Microstructure. *Polymers* **2017**, *9*, 164. https://doi.org/10.3390/polym9050164

(55) Grabber, J. H.; Ralph, J.; Hatfield, R. D. Ferulate Cross-Links Limit the Enzymatic Degradation of Synthetically Lignified Primary Walls of Maize. *J. Agric. Food Chem.* **1998**, *46* (7), 2609–2614. https://doi.org/10.1021/jf9800099

(56) Grabber, J. H.; Hatfield, R. D.; Ralph, J. Diferulate Cross-Links Impede the Enzymatic Degradation of Non-Lignified Maize Walls. *J. Sci. Food Agric.* **1998**, *77*, 193–200. https://doi.org/ 10.1002/(SICI)1097-0010(199806)77:2<193::AID-JSFA25>3.0.CO;2-A.

(57) Mnich, E.; Bjarnholt, N.; Eudes, A.; Harholt, J.; Holland, C.; Jørgensen, B.; Larsen, F. H.; Liu, M.; Manat, R.; Meyer, A. S.; et al. Phenolic Cross-Links: Building and de-Constructing the Plant Cell Wall. *Nat. Prod. Rep.* **2020**, https://doi.org/10.1039/c9np00028c.

(58) Verbruggen, M.; Spronk, B.; Schols, H. A.; Beldman, G.; Voragen, A. G. J.; Thomas, J.; Kamerling, J. P.; Vliegenthart, J. F. G. Structures of Enzymically Derived Oligosaccharides from Sorghum Glucuronoarabinoxylan. *Carbohydr. Res.* **1998**, *306*, 265–274. https://doi.org/10.1016/S0008-6215(97)10064-7

(59) Channe Gowda, D.; Sarathy, C. Structure of an L-Arabino-D-Xylan from the Bark of *Cinnamomum zeylanicum*. *Carbohydr. Res.* **1987**, *166* (2), 263–269. https://doi.org/10.1016/0008-6215(87)80062-9.

(60) Cardoso, S.; Ferreira, J.; Mafra, I.; Silva, A.; Coimbra, M. Structural Ripening-Related Changes of the Arabinan-Rich Pectic Polysaccharides from Olive Pulp Cell Walls. *J. Agric. Food Chem.* **2007**, *55* (17), 7124–7130. https://doi.org/10.1021/jf070769w.

(61) Naran, R.; Black, S.; Decker, S. R.; Azadi, P. Extraction and Characterization of Native Heteroxylans from Delignified Corn Stover and Aspen. *Cellulose* **2009**, *16* (4), 661–675. https://doi.org/10.1007/s10570-009-9324-y.

(62) Biely, P.; Vršanská, M.; Tenkanen, M.; Kluepfel, D. Endo-β-1,4-Xylanase Families: Differences in Catalytic Properties. *J. Biotechnol.* **1997**, *57*, 151–166. https://doi.org/10.1016/S0168-1656(97)00096-5.

(63) Pozdnyakova, N. N.; Turkovskaya, O. V; Yudina, E. N.; Rodakiewicz-Nowak, Y. Yellow Laccase from the Fungus *Pleurotus ostreatus* D1: Purification and Characterization. *Appl. Biochem. Microbiol.* **2006**, *42* (1), 56–61. https://doi.org/10.1134/S000368380601008X.

(64) Pozdnyakova, N. N.; Rodakiewicz-Nowak, J.; Turkovskaia, O. V. Catalytic Properties of Yellow Laccase from *Pleurotus ostreatus* D1. *J. Mol. Catal. B Enzym.* **2004**, *30*, 19–24. https://doi.org/10.1016/j.molcatb.2004.03.005.

(65) Hollmann, F.; Gumulya, Y.; Tölle, C.; Liese, A.; Thum, O. Evaluation of the Laccase from *Myceliophthora thermophila* as Industrial Biocatalyst for Polymerization Reactions. *Macromolecules* **2008**, *41* (22), 8520–8524. https://doi.org/10.1021/ma801763t.

(66) Munk, L.; Andersen, M. L.; Meyer, A. S. Direct Rate Assessment of Laccase Catalysed Radical Formation in Lignin by Electron Paramagnetic Resonance Spectroscopy. *Enzyme Microb. Technol.* **2017**, *106*, 88–96. http://doi.org/10.1016/j.enzmictec.2017.07.006.

(67) Berka, R. M.; Schneider, P.; Golightly, E. J.; Brown, S. H.; Madden, M.; Brown, K. M.; Halkier, T.; Mondorf, K.; Xu, F. Characterization of the Gene Encoding an Extracellular Laccase of *Myceliophthora thermophila* and Analysis of the Recombinant Enzyme Expressed in *Aspergillus oryzae*. *Appl. Environ. Microbiol.* **1997**, *63* (8), 3151–3157. https://doi.org/10.1128/AEM.63.8.3151-3157.1997.

TOC graphic

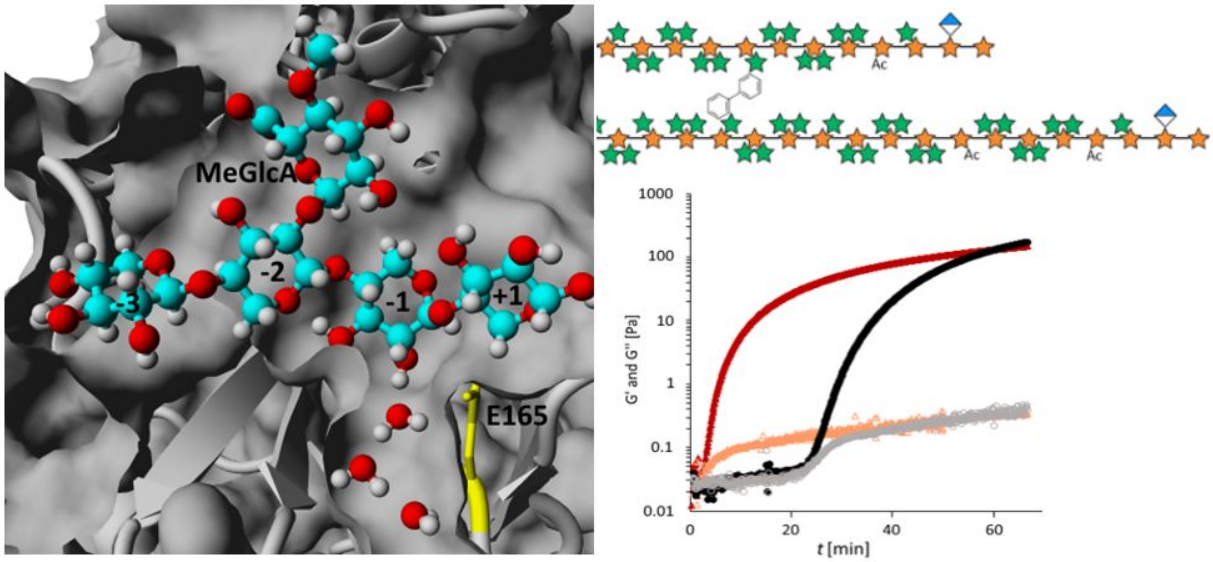

SYNOPSIS: A GH30 xylanase from *Dickeya chrysanthemi* was used to extract cross-linkable, highly feruloylated, high-molecular weight glucuronoarabinoxylan from corn bran.